

The coordination behaviour of 2-((*E*)-(tert-butylimino)methyl)phenol towards lanthanide nitrate and chloride salts

Kwakhanya Mkwakwi, Eric C. Hosten , Richard Betz, Abubak'r Abrahams  and Tatenda Madanhire* 

Department of Chemistry, Nelson Mandela University, Port Elizabeth, South Africa

ABSTRACT

Five novel complexes were prepared by reacting 2-((*E*)-(tert-butylimino)methyl)phenol (HL₂) with Ln(NO₃)₃·*x*H₂O (Ln = Gd and Dy; *x* = 6 and 5, respectively) and LnCl₃·6H₂O (Ln = Nd, Gd and Dy). The crystal structures of the former two Ln(III) nitrate complexes are isostructural and the coordination sphere is composed of three monodentate HL₂ ligands bonded to the metal centre through the phenolic oxygen atom and three nitrate ions coordinated in a bidentate fashion. Both complexes are nine-coordinate and *SHAPE* analysis reveals that they adopted a muffin polyhedra geometric type. The average Ln–O_{nitrate} and Ln–O_{phenolate} bond lengths are 2.5059 and 2.2816 Å, respectively. The complexes derived from the chloride salts exhibited an octahedral geometry with four monodentate Schiff base ligands [Ln–O_{phenolate} distances range from 2.229(4) to 2.2797(18) Å] coordinating in the equatorial positions and two chloride ions [average Ln–Cl bond length is 2.6530 Å, and average Cl–Ln–Cl angles is 180°] in axial positions. The ligand coordinated through the phenolate oxygen with the phenolic proton migrating to the imino nitrogen to give a zwitterionic form of the ligand. There are weak C–H...Cl interactions present and O–H...N hydrogen bonds are also observed in the crystal packing.

KEYWORDS

bidentate, lanthanide, monodentate, Schiff base, zwitterion

Received 21 August 2022, revised 17 January 2023, accepted 19 January 2023

INTRODUCTION

Schiff bases and their complexes have been investigated for their interesting and important properties, such as their ability to reversibly bind oxygen and their catalytic activity in the hydrogenation of olefins.^{1,2} Schiff bases also display biological activity such as antibacterial, antifungal, antitumour and antioxidant properties.³ On an industrial scale, these versatile ligands are used as pigments and dyes. They are also able to stabilize oxidation states of different metals, therefore controlling the performance of metals in numerous catalytic transformations.⁴

The *d*- and *f*-block metal coordination compounds containing phenolate ligands have been studied due to their interesting properties, such as luminescence and catalytic activities.^{5,6} Complexation studies of 2-(2'-hydroxyphenyl)benzimidazole (HPBI) with Nd(NO₃)₃·6H₂O and YbCl₃·6H₂O to yield two complexes, (H₂PBI)₂[Nd(HPBI)₂(NO₃)₄]₂·2CH₃OH·2H₂O and (H₂PBI)[Yb(HPBI)₂Cl₄]₂·2CH₃OH indicated monodentate binding of HPBI.⁵ The unit cell of the neodymium complex consisted of two [Nd(HPBI)₂(NO₃)₄][−] units with each Nd³⁺ ion being ten-coordinate, with two phenolate oxygen atoms of the ligand and eight oxygen donor atoms from four bidentate nitrate ions surrounding the metal. Structural analysis of the ytterbium complex indicated that the Yb³⁺ ion is lying on an inverse centre and is connected to two phenolate oxygen atoms donated from two ligands and four chloride ions. The resulting six-coordinate complex adopts an octahedral geometry. One protonated ligand is also present to balance the charge of the [Yb(HPBI)₂Cl₄][−] unit. It was also reported that both complexes displayed near-infrared luminescence which is characteristic of Nd³⁺ and Yb³⁺ ions.⁵

Khorshidifard *et al.* reported transition metal complexes with the potentially bidentate *N,O*-donor ligand 2-*tert*-butyliminomethylphenol (HL₂, Figure 1a), as depicted in Figure 1b.⁶ Crystallographic data revealed that two Schiff base ligands coordinated to the metal centre *via* the two phenolate oxygen and the two imino nitrogen atoms. The

geometries around the metal centres in the CoL₂, CuL₂ and ZnL₂ complexes were distorted tetrahedron, while the palladium complex adopted a square-planar geometry. It was found that these complexes promoted the oxidation of thionisole to the corresponding sulfone and sulfoxide. Several factors were found to influence the reaction, *viz.* the reaction temperature, the geometrical structure of the catalyst and the oxidation of different sulphides. The ZnL₂ complex was found to display the best catalyst activity. It was proposed that the low catalytic activity of the CoL₂ complex was due to the geometry of the ligands, which increased steric hindrance, and thus lowered the accessibility of the metal centre in the catalyst.⁶

Lanthanide chloride complexes would be expected to be better catalysts compared to their nitrate counterparts. This could be attributed to the fact that the coordination sphere of lanthanide nitrate complexes tends to be more saturated compared to the chloride complexes, because the oxygen donor-atoms of the nitrate ions are more electronegative than the chloride ions, making them harder to substitute during catalytic processes. The catalytic performance of a complex has been proposed to be dependent on the steric congestion around the metal centre.^{7,8}

Herein, we report the reactions of the Schiff base ligand HL₂ derived from *tert*-butylamine with Ln(NO₃)₃·*x*H₂O (Ln = Gd and Dy) and LnCl₃·*x*H₂O (Ln = Nd, Gd and Dy) to yield [Ln(NO₃)₃(HL₂)₃] and

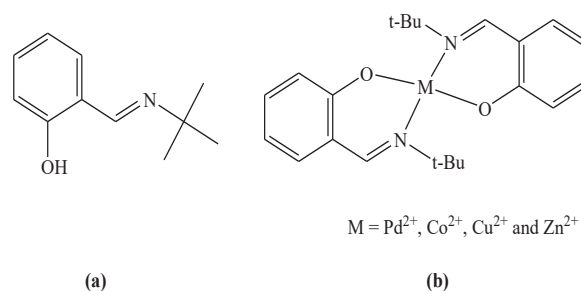


Figure 1: (a) Chemical structure of HL₂; (b) Structural formula of the four-coordinate transition metal complexes with HL₂

*To whom correspondence should be addressed
Email: Tatenda.Madhanhire@mandela.ac.za

[Ln(Cl)₂(HL₂)₄]Cl, as well as the structure determinations of these compounds.

EXPERIMENTAL

Chemicals and instrumentation

The solvents used in this study were purchased from Merck: methanol, ethanol, acetonitrile, iso-propanol, dichloromethane, dimethyl sulfoxide and diethyl ether, while dimethyl formamide was purchased from Sigma-Aldrich, and used without further purification. The deuterated solvents used in NMR spectroscopy (CDCl₃ and DMSO-*d*₆) were purchased from Merck. The hydrated lanthanide nitrates, Gd(NO₃)₃·6H₂O (99.9%) and Dy(NO₃)₃·5H₂O (99.0%), as well as LnCl₃·6H₂O [Ln = Nd (99.9%), Gd (99.9%) and Dy (99.0%)] were sourced from Sigma-Aldrich. Salicylaldehyde (98.0%) and *tert*-butylamine (99.0%) used in the synthesis of HL₂ were sourced from Sigma-Aldrich and Riedel-de Haën, respectively.

A Bruker Tensor 27 FT-IR spectrophotometer, equipped with the Platinum ATR attachment was used to obtain the infrared spectra of the compounds. The samples were run neat on ATR and the recorded data analysed with *OPUS 6.5* software. The UV-Vis spectra were done on a PerkinElmer Lambda 35 UV-Vis spectrophotometer and processing performed using *UV WinLab* software. Nuclear Magnetic Resonance (NMR) spectra were recorded using a Bruker AvanceIII 400 NMR Spectrometer at 295K and acquisition of data done using *TopSpin 3.0* software. The *ACD/Labs* software was used in the analysis of the NMR spectra.

A Bruker APEX II X-ray Crystallography System was utilized in single-crystal diffractometry at 200 K ($\lambda = 0.71073 \text{ \AA}$). The *SAINT*

software was used for data reduction and cell refinement.⁹ The structures were solved and refined using *SHELXS97* and *SHELXL97* software, respectively.^{10,11} Molecular graphics were obtained using *ORTEP III* for Windows.¹² The coordination geometries of the Ln(III) complexes were evaluated using *SHAPE 2.1* software and polyhedral representations created using *VESTA* software. Table 1 gives a summary of the crystal data and parameters for data collection and refinement for complexes 1–5.

Synthesis of 2-((E)-(tert-butylimino)methyl)phenol (HL₂)

The synthesis of HL₂ was carried out using a literature procedure.¹³ A solution of salicylaldehyde (2.44 g, 20.0 mmol) was added to a solution of 1.47 g of *tert*-butylamine (20.1 mmol) in 20 ml methanol. The resulting yellow mixture was stirred at room temperature for 1 hr. After the removal of the solvent under vacuum, a yellow oil was obtained. Yield: 96.0 %. UV-Vis (DMF, λ_{max} nm (ϵ , M⁻¹cm⁻¹): 279 (3466) 361 (5210), 402 (2332). IR (cm⁻¹): ν (C-H) 3034, 2974, 2918(w); ν (C=N) 1628(s); ν (C_{ph}-O) 1281(s). ¹H NMR (CDCl₃, δ ppm): 8.52 (s, 1H, HC=N), 7.45-7.43 (d, 1H, Ar), 7.34-7.30 (t, 1H, Ar), 6.95-6.93 (d, 1H, Ar), 6.91-6.87 (t, 1H, Ar), 2.00 (s, 1H, -OH), 1.31 (s, 9H, -CH₃).

Synthesis of the metal complexes

Synthesis of [Gd(NO₃)₃(HL₂)₃] (1)

A 10 ml solution of HL₂ in methanol (0.531g, 3.00 mmol) was carefully transferred to a 10 ml methanolic solution of Gd(NO₃)₃·6H₂O (0.452 g, 1.00 mmol). The two solutions were allowed to diffuse slowly at 0 °C, and X-ray quality single crystals grew within 2 days. Yield = 75.7 %, m.p. = 200 °C (decomposition). Anal. Cald for C₃₃H₄₅GdN₆O₁₂ (%): C,

Table 1: Crystal and structure refinement data for complexes 1–5

Complex	1	2	3	4	5
Formula	C ₃₃ H ₄₅ GdN ₆ O ₁₂	C ₃₃ H ₄₅ DyN ₆ O ₁₂	C ₄₄ H ₆₀ Cl ₃ N ₄ NdO ₄	C ₄₄ H ₆₀ Cl ₃ GdN ₄ O ₄	C ₄₄ H ₆₀ Cl ₃ DyN ₄ O ₄
M _r (g.mol ⁻¹)	875.00	880.25	959.55	972.56	977.81
Crystal system	Trigonal	Trigonal	Orthorhombic	Orthorhombic	Orthorhombic
Space group	R-3 (No.148)	R-3 (No.148)	<i>Pnc2</i> (No. 30)	<i>Pnc2</i> (No. 30)	<i>Pnc2</i> (No. 30)
a (Å)	48.5479(14)	48.3719(11)	11.7852(3)	11.7823(4)	11.743(1)
b (Å)	48.5479(14)	48.3719(11)	11.7459(3)	11.7428(4)	11.7302(10)
c (Å)	10.4575(3)	10.4574(3)	17.3612(5)	17.3550(5)	17.3391(15)
α (°)	90	90	90	90	90
β (°)	90	90	90	90	90
γ (°)	120	120	90	90	90
V (Å ³)	21345.2(14)	21190.5(11)	2403.27(11)	2401.19(13)	2388.4(4)
Z	18	18	2	2	2
ρ (g.cm ⁻³)	1.225	1.242	1.326	1.345	1.360
μ (mm ⁻¹)	1.452	1.641	1.289	1.590	1.774
F(000)	8010	8046	990	998	1002
Crystal size (mm ³)	0.16×0.18×0.37	0.09×0.10×0.41	0.11×0.52×0.58	0.16×0.17×0.22	0.24×0.54×0.56
θ (min-max) (°)	2.3, 28.3	2.5, 28.3	2.4, 28.3	2.4, 28.4	1.7, 28.4
Data set	-64≤h≤62 -64≤k≤64 -13≤l≤13	-64≤h≤63 -64≤k≤59 -13≤l≤13	-15≤h≤15 -15≤k≤15 -23≤l≤23	-15≤h≤15 -15≤k≤15 -15≤l≤23	-15≤h≤15 -15≤k≤15 -23≤l≤23
Tot., Unique data, R _{int}	255900, 11787, 0.030	69003, 11720, 0.041	31822, 5915, 0.018	21158, 4767, 0.016	148657, 5946, 0.037
Observed [I>2 σ (I)] reflections	10356	9199	4554	3855	4691
N _{reflections} N _{parameters}	11787, 482	11720, 482	5915, 270	4767, 269	5946, 263
R[F ² >2 σ (F ²)], wR(F ²), S	0.0262, 0.0767, 1.05	0.0285, 0.0690, 1.04	0.0250, 0.0605, 1.12	0.0161, 0.0395, 1.05	0.0331, 0.0775, 1.22
$\Delta\rho_{\text{min}}$, $\Delta\rho_{\text{max}}$ (e.Å ⁻³)	-0.56, 0.61	-0.50, 0.57	-0.43, 0.71	-0.22, 0.23	-0.78, 1.25

45.30; H, 5.18; N, 9.60. Found: C, 45.14; H, 5.13; N, 9.52. Conductivity (10^{-3} M, DMF): $143.0 \text{ ohm}^{-1}\text{cm}^2\text{mol}^{-1}$. UV-Vis (DMF, λ_{max} nm (ϵ , $\text{M}^{-1}\text{cm}^{-1}$): 256 (13218), 315 (12368), 383 (2544). IR (cm^{-1}): $\nu(\text{C-H})$ 2978, 2943, 2913, 2874(w); $\nu(\text{C=N})$ 1636(s); $\nu_1(\text{NO}_3^-)$ 1286(s); $\nu_4(\text{NO}_3^-)$ 1474(s); $\nu_2(\text{NO}_3^-)$ 1032(m); $\nu_6(\text{NO}_3^-)$ 818(w); $\nu(\text{Gd-O})$ 477(w).

Synthesis of $[\text{Dy}(\text{NO}_3)_3(\text{HL}_2)_3]$ (2)

The synthesis protocol used in **1** was adopted in the reaction of $\text{Dy}(\text{NO}_3)_3 \cdot 5\text{H}_2\text{O}$ (0.438 g, 0.999 mmol) and HL_2 (0.531g, 3.00 mmol) in methanol. Yellow, single crystals suitable for X-ray analysis were obtained within 48 hrs. Yield = 26.4 %, m.p. = 170 °C (decomposition). Anal. Cald for $\text{C}_{33}\text{H}_{45}\text{DyN}_6\text{O}_{12}$ (%): C, 45.03; H, 5.15; N, 9.55. Found: C, 45.09; H, 5.08; N, 9.50. Conductivity (10^{-3} M, DMF): $96.8 \text{ ohm}^{-1}\text{cm}^2\text{mol}^{-1}$. UV-Vis (DMF, λ_{max} nm (ϵ , $\text{M}^{-1}\text{cm}^{-1}$): 266 (10186), 315 (9594), 383 (2188). IR (cm^{-1}): $\nu(\text{C-H})$ 2980, 2961, 2916(w); $\nu(\text{C=N})$ 1637(s); $\nu_1(\text{NO}_3^-)$ 1288(s); $\nu_4(\text{NO}_3^-)$ 1447(s); $\nu_2(\text{NO}_3^-)$ 1034(m); $\nu_6(\text{NO}_3^-)$ 825(w); $\nu(\text{Dy-O})$ 477(w).

Synthesis of $[\text{Nd}(\text{Cl})_2(\text{HL}_2)_4]\text{Cl}$ (3)

To a 10 ml methanolic solution of $\text{NdCl}_3 \cdot 6\text{H}_2\text{O}$ (0.358 g, 0.998 mmol) was added a 10 ml solution of HL_2 (0.708 g, 3.99 mmol). Diethyl ether was diffused into the resulting solution at 0 °C and single crystals grew within 24 hrs. Yield = 32.5 %, m.p. = 246 °C. Anal. Cald for $\text{C}_{44}\text{H}_{60}\text{Nd}_4\text{NdO}_4\text{Cl}_3$ (%): C, 55.07; H, 6.30; N, 6.67. Found: C, 55.12; H, 6.38; N, 6.60. Conductivity (10^{-3} M, DMF): $105 \text{ ohm}^{-1}\text{cm}^2\text{mol}^{-1}$. UV-Vis (DMF, λ_{max} nm (ϵ , $\text{M}^{-1}\text{cm}^{-1}$): 265 (13644), 314 (12976), 395(1090). IR (cm^{-1}): $\nu(\text{C-H})$ 2974, 2929, 2893, 2871(w); $\nu(\text{C=N})$ 1639(s); $\nu(\text{C}_{\text{ph}}-\text{O})$ 1299(m); $\nu(\text{Nd-O})$ 476(m); $\nu(\text{Nd-Cl})$ 374(m).

Synthesis of $[\text{Gd}(\text{Cl})_2(\text{HL}_2)_4]\text{Cl}$ (4)

The same experimental protocol used in **3** was adopted. Yellow, single crystals suitable for X-ray crystallography were obtained from the reaction between $\text{GdCl}_3 \cdot 6\text{H}_2\text{O}$ (0.371 g, 0.998 mmol) and HL_2 (0.708 g, 3.99 mmol). Yield = 39.8 %, m.p. = 213 °C. Anal. Cald for $\text{C}_{44}\text{H}_{60}\text{GdN}_4\text{O}_4\text{Cl}_3$ (%): C, 54.34; H, 6.22; N, 5.76. Found: C, 54.32; H, 6.20; N, 5.78. Conductivity (10^{-3} M, DMF): $58.4 \text{ ohm}^{-1}\text{cm}^2\text{mol}^{-1}$. UV-Vis (DMF, λ_{max} nm (ϵ , $\text{M}^{-1}\text{cm}^{-1}$): 265 (12082), 314 (11714), 400 (996). IR (cm^{-1}): $\nu(\text{C-H})$ 2974, 2930, 2852(w); $\nu(\text{C=N})$ 1639(s); $\nu(\text{C}_{\text{ph}}-\text{O})$ 1300(m); $\nu(\text{Gd-O})$ 474(m), $\nu(\text{Gd-Cl})$ 375(m).

Synthesis of $[\text{Dy}(\text{Cl})_2(\text{HL}_2)_4]\text{Cl}$ (5)

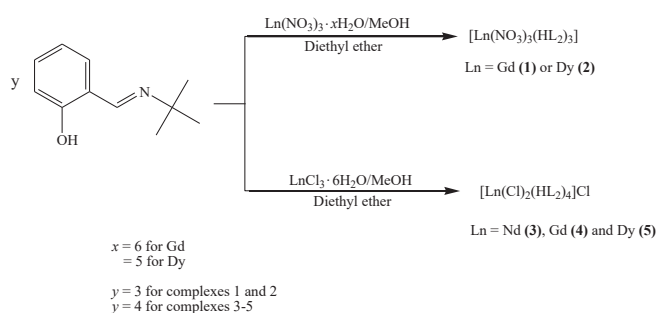
The synthesis method employed in **1** was replicated in the reaction between $\text{DyCl}_3 \cdot 6\text{H}_2\text{O}$ (0.376 g, 0.997 mmol) and HL_2 (0.708 g, 3.99 mmol), which yielded yellow X-ray quality crystals. Yield = 38.4%, m.p. = 274 °C (decomposition). Anal. Cald for $\text{C}_{44}\text{H}_{60}\text{Cl}_3\text{DyN}_4\text{O}_4$ (%): C, 54.05; H, 6.18; N, 5.73. Found: C, 53.98; H, 6.14; N, 5.68. Conductivity (10^{-3} M, DMF): $132.6 \text{ ohm}^{-1}\text{cm}^2\text{mol}^{-1}$. UV-Vis (DMF, λ_{max} nm (ϵ , $\text{M}^{-1}\text{cm}^{-1}$): 266 (12354), 325 (10442), 370 (1964) IR (cm^{-1}): $\nu(\text{C-H})$ 2999, 2980(w), $\nu(\text{C=N})$ 1621(s), $\nu(\text{C}_{\text{ph}}-\text{O})$ 1303(m), $\nu(\text{Dy-O})$ 476(m), $\nu(\text{Dy-Cl})$ 404(m).

RESULTS AND DISCUSSION

Synthesis and spectral characterization

The synthesis of complexes **1** and **2** was carried out by reacting lanthanide nitrate salts and HL_2 in a 1:3 molar ratio in methanol as illustrated in Scheme 1. The reaction of $\text{Nd}(\text{NO}_3)_3 \cdot 6\text{H}_2\text{O}$ with HL_2 yielded thin flexible fibers which could not be analyzed crystallographically. Complexes **3-5** were prepared from the reactions of lanthanide chloride salts and HL_2 (Scheme 1). X-ray quality crystals of **1-5** were obtained by vapour diffusion using diethyl ether at 0 °C.

The complexes are non-hygroscopic, crystalline solids which are air stable for months. All the compounds are partially soluble in methanol



Scheme 1: Synthetic procedures of complexes 1–5

and ethanol, insoluble in acetonitrile, iso-propanol, dichloromethane and water, and soluble in dimethyl formamide and dimethyl sulfoxide. Complexes **1**, **2** and **5** decomposed on heating in the temperature range 170–274 °C, while complexes **3** and **4** melted at 246 and 213 °C, respectively. The molar conductivity of 10^{-3} M DMF solutions of **1-5** lies between 58.4 and $143.0 \text{ ohm}^{-1}\text{cm}^2\text{mol}^{-1}$. According to W.J. Geary, acceptable molar conductivity ranges of 1:1 and 2:1 electrolyte types in DMF are 65–90 and $130\text{--}170 \text{ ohm}^{-1}\text{cm}^2\text{mol}^{-1}$, respectively.¹⁴ Complex **4** falls short of the 1:1 electrolyte range, while **2** and **3** fall within the range, which confirms the two chloride ions inside and the one chloride outside the coordination sphere.¹⁵ Complexes **1** and **5** fall within the 2:1 electrolyte type range. The unexpectedly high conductivity values of neutral complexes **1** and **2** could be a result of the zwitterionic effect of the ligands.¹⁶

In the IR spectrum of HL_2 (Figure S1a; in supplementary information), the sharp band observed at 1628 cm^{-1} is characteristic of the $>\text{C}=\text{N}$ - functional group stretch, and in **1** and **2** (Figure S1b), this band appears at $ca 1636 \text{ cm}^{-1}$, a shift of about $+8 \text{ cm}^{-1}$. The spectrum of the free ligand also displays a band at 1281 cm^{-1} , which is assigned to the phenolic C-O group vibration. The band corresponding to the phenolic $\nu(\text{C-O})$ shifted to a higher wavenumber ($\sim 1286 \text{ cm}^{-1}$), which is attributed to the formation of the metal-oxygen bond. The four bands attributed to the vibrations of the coordinated nitrate groups were observed at approximately $1481(\nu_4)$, $1286(\nu_1)$, $1032(\nu_2)$ and $818(\nu_6) \text{ cm}^{-1}$. The difference between ν_4 and ν_1 (195 cm^{-1}) confirms the bidentate nature of the NO_3^- groups.^{14,15} The infrared spectra of **3**, **4** and **5** (Figure S1c) presents the azomethine vibrational bands at about $1621\text{--}1639 \text{ cm}^{-1}$. The C-O stretches exhibited a blue shift in the range $1299\text{--}1303 \text{ cm}^{-1}$ in the spectra of the complexes; this confirms the coordination of phenolic oxygens to the metal ions. The new bands appearing at $476\text{--}478 \text{ cm}^{-1}$ in **1-5** are assigned to $\nu(\text{Ln-O})$.^{8,15,17}

The ^1H NMR spectrum of HL_2 in CDCl_3 (Figure S2a; see Figure S2b for ^{13}C spectrum) shows a singlet at 8.52 ppm, which is attributed to the azomethine proton H7. The doublet at 7.45–7.43 ppm, the triplet at 7.31–7.30 ppm, the doublet at 6.95–6.93 ppm and the triplet at 6.89–6.87 ppm are assigned to protons H5, H3, H2 and H4, respectively. The phenolic proton appeared as a singlet at 2.00 ppm. The resonance at 1.31 ppm integrating to nine protons is assigned to the *tert*-butyl protons of HL_2 . In the ^1H spectrum of **1** (Figure S2c), in $\text{DMSO-}d_6$, the singlet at 14.40 ppm is assigned to the zwitterionic (N-H) proton, while the signals appear at 14.34 ppm in **3** and **4** (Figures S2d and S2e). Upon complexation, the azomethine proton resonance shifted up-field to 8.59 ppm in **1**. The azomethine proton resonances are observed at 8.56 and 8.57 ppm in **3** and **4**, respectively, with shifts of 0.04 and 0.05 ppm, respectively, from the free ligand. The aromatic protons resonance range lies between 7.74–6.87 ppm and the chemical shift attributed to the *tert*-butyl protons appear at 1.30 ppm in **1**, **3** and **4**.

The paramagnetic nature of complexes **1**, **3** and **4** creates lanthanide induced shifts (LIS), which causes the proton resonances of the ligand to shift upon coordination. The LIS depends on the paramagnetic anisotropy of the Ln(III) ion, the geometrical position of the nucleus within the complex and the distance of the ligand's proton from the paramagnetic ion.¹⁸ The NMR data reveals that the *tert*-butyl protons

experience a lesser shift, because of their special proximity to the nucleus. The NMR spectra of **1** and **4** also display signal broadening, which is attributed to the increased nuclear relaxation induced by the electronic magnetic moment.¹⁹ However, the proton spectrum of **3** exhibited no line-broadening.

The overlay UV-Vis spectra of the free ligand and complexes **1** and **2** were recorded in DMF (Figure 2a). The intense band at 265 nm in the free ligand is due to $\pi \rightarrow \pi^*$ transitions of the benzene ring. The bands at 315 nm and 400 nm are attributed to the $\pi \rightarrow \pi^*$ and $n \rightarrow \pi^*$ transitions of the phenolic -OH and the azomethine moieties, respectively.²⁰ The electronic spectra of **1** and **2** exhibited absorption bands similar to those of the free ligand; these bands are observed at about 265, 315 and 383 nm. The first two bands remained unaffected by coordination, whilst the last absorption band shifted to a lower wavelength. The spectra of complexes **3** and **5** (Figure 2b) are dominated by the bands of the ligand; the electronic transitions being observed at 265 and 314 nm. A third absorbance band in **3** and **4** appeared at 395 and 400 nm, respectively. Complex **5** displays three transitions at 266, 325 and 370 nm. The absorption bands of the ligand are shifted slightly upon complexation, which are due to changes in the energy levels of the ligand orbitals.²¹

Crystal structure

X-ray crystallographic analysis reveals that both **1** and **2** crystallized as monomeric complexes with the general formula $[\text{Ln}(\text{HL}_2)_3(\text{NO}_3)_3]$ [$\text{Ln} = \text{Gd}$ (**1**) and Dy (**2**)], in the trigonal $R\bar{3}$ space group with unit cell parameters: [$a = 48.5479(14)$, $b = 48.5479(14)$, $c = 10.4575(3)$, $\alpha = \beta = 90^\circ$, $\gamma = 120^\circ$, $V = 21345.2(14) \text{ \AA}^3$ and $Z = 18$ for **1**, and $a = b = 48.3719(11)$, $c = 10.4574(3)$, $\alpha = \beta = 90^\circ$, $\gamma = 120^\circ$, $V = 21190.5(11) \text{ \AA}^3$ and $Z = 18$ for **2**]. The metal ions are nine-coordinate with three oxygen atoms originating from three monodentate HL_2 ligands and three bidentate nitrate ions (Figure 3). The geometries of the GdO_9 and DyO_9 coordination polyhedra of the metal complexes with the Schiff base were determined by continuous shape measures (CShMs) using

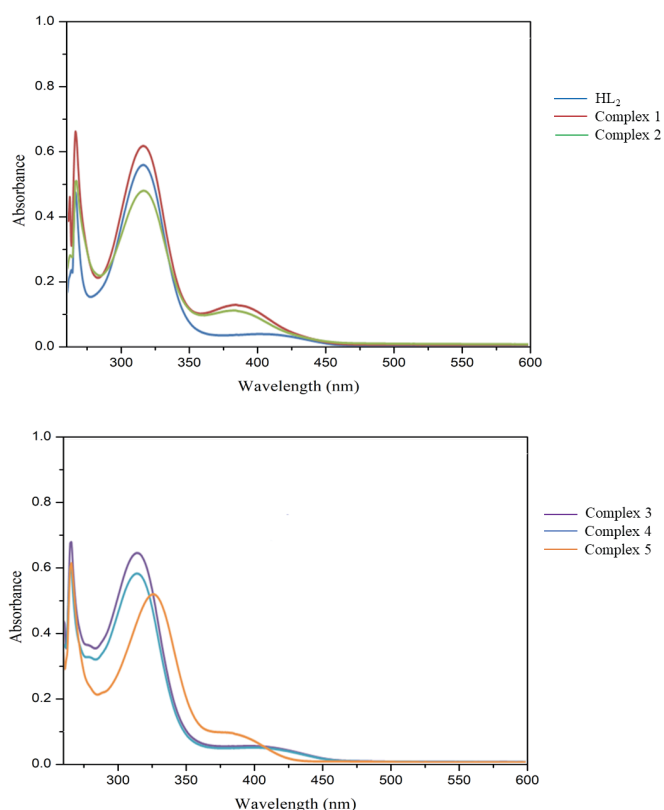


Figure 2: (a) Electronic spectra of HL_2 , **1** and **2** (1×10^{-3} DMF solution) (b) UV-Vis spectra of **3**, **4** and **5** in DMF

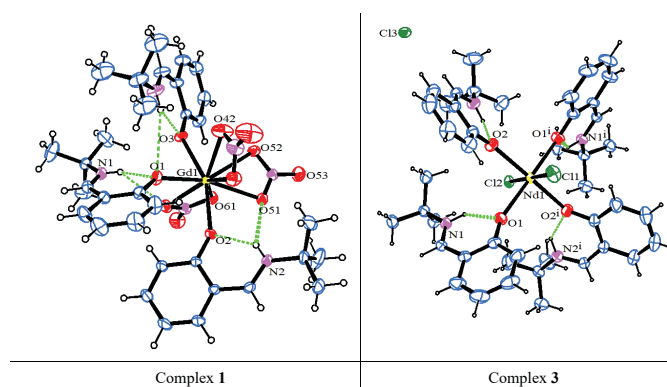


Figure 3: The crystal structures of complexes **1** and **3**, showing partial atom-numbering and hydrogen bonding (dashed green lines) (30% probability displacement ellipsoids).

Table 2: Continuous Shape Measurement values of 1–5.

Shape	Symmetry	CShM values		
		Complex 1	Complex 2	
Enneagon (EP-9)	D_{9h}	33.565	33.463	
Octagonal pyramid (OPY-9)	C_{8v}	22.764	22.649	
Heptagonal bipyramid (HBPY-9)	D_{7h}	17.853	18.095	
Spherical-relaxed capped cube (CCU-9)	C_{4v}	8.834	9.088	
Spherical capped square antiprism (CSAPR-9)	C_{4v}	2.776	2.657	
Spherical tricapped trigonal prism (TCTPR-9)	D_3	4.080	3.904	
Hula-hoop (HH-9)	C_{2v}	9.283	9.642	
Muffin (MFF-9)	C_s	2.472	2.379	
		Complex 3	Complex 4	Complex 5
Hexagon (HP-6)	D_{6h}	32.959	32.935	32.979
Pentagonal pyramid (PPY-6)	C_{5v}	29.575	29.567	29.602
Octahedron (OC-6)	O_h	0.625	0.630	0.671
Trigonal prism (TPR-6)	D_{3h}	17.050	17.042	17.066

Note: Relative path-deviation functions: Complexes **3** and **4** = 12.2%; Complex **5** = 12.7%

SHAPE 2.1 software (Table 2). The coordination geometries of the nine-coordinate complexes **1** and **2** are classified as distorted muffin (MFF-9), with CShM values of 2.472 and 2.379, respectively (Figure 4). The relative path-deviation functions for complexes **1** and **2** are 19.3 and 18.7%, respectively. The imino nitrogen remained uncoordinated, and the Schiff base ligands in the complexes exist in their zwitterionic forms (upon complexation the phenolic proton was transferred to the imino nitrogen atom). This is similar to the monomeric nine-coordinate neodymium salicylaldehyde coordination polymer described by the formula $[\text{Nd}_2(\text{H}_2\text{salen})_3(\text{NO}_3)_6]_n$.²²

The bond parameters of complexes **1**–**5** are listed in Table 3. The average $\text{Ln}-\text{O}_{\text{nitrate}}$ bond lengths in **1** = 2.5166 and **2** = 2.4952 Å. These values compare well with the similar complex $(\text{H}_2\text{PBI})_2[\text{Nd}(\text{HPBI})_2(\text{NO}_3)_4] \cdot 2\text{CH}_3\text{OH} \cdot 2\text{H}_2\text{O}$ (average $\text{Ln}-\text{O}_{\text{nitrate}}$ = 2.5675 Å).⁵ The average $\text{Ln}-\text{O}_{\text{phenolate}}$ bond lengths in **1** and **2** are 2.2986 and 2.2646 Å, respectively. In the Nd salicylaldehyde complex, the average $\text{Nd}-\text{O}_{\text{phenolate}}$ bond length is 2.3443 Å.²² The shorter $\text{Ln}-\text{O}_{\text{phenolate}}$ bond lengths compared to the $\text{Ln}-\text{O}_{\text{nitrate}}$ bond distances are due to more resonance delocalization of electrons (more stability) in the phenolate moiety compared to the nitrate ion. The shorter $\text{Ln}-\text{O}$ bond distances in **2** compared to **1** is attributed to the lanthanide contraction. The $\text{Ln}-\text{O}$ distances are all within and similar to those

Table 3: Selected bond distances (Å) and angles (°) in **1–5**.

	1 [Gd]	2 [Dy]	3 [Nd]	4 [Gd]	5 [Dy]	
Bond lengths (Å)						
Ln-O1	2.3108(18)	2.246(2)	Ln-Cl1	2.636(4)	2.627(2)	2.615(4)
Ln-O2	2.283(2)	2.2859(17)	Ln-Cl2	2.683(2)	2.695(2)	2.662(4)
Ln-O3	2.302(2)	2.262(2)	Ln-O1	2.264(4)	2.2643(18)	2.229(4)
Ln-O41	2.523(3)	2.485(2)	Ln-O2	2.278(3)	2.2797(18)	2.250(4)
Ln-O42	2.539(3)	2.4493(19)	Ln-O1a	2.264(4)	2.2643(18)	2.229(4)
Ln-O51	2.4895(18)	2.498(2)	Ln-O2a	2.278(3)	2.2797(18)	2.250(4)
Ln-O52	2.567(2)	2.522(2)	N2-C21	1.276(7)	1.285(4)	1.273(9)
Ln-O61	2.474(2)	2.471(2)	O1-C112	1.318(6)	1.309(3)	1.301(9)
Ln-O62	2.507(2)	2.546(2)				
Bond angles (°)						
O41-Ln-O42	49.49(8)	51.59(6)	O1-Ln-O1a	175.5(2)	175.16(11)	176.1(3)
O51-Ln-O52	49.66(6)	50.02(9)	O2-Ln-O2a	175.4(2)	174.98(11)	175.6(3)
O61-Ln-O62	51.22(7)	50.12(8)	Cl1-Ln-Cl2	180.00	180.00	180.00
N1-C11-C111	125.2(2)	125.0(3)	N1-C11-C111	123.2(4)	123.5(2)	122.6(6)
N2-C21-C211	125.1(2)	125.1(3)	N2-C21-C211	124.6(5)	124.3(3)	125.8(7)
N3-C31-C311	125.6(3)	126.2(3)				

observed for analogous complexes [Ln-O bond lengths ranges from 2.412–2.492 Å].^{23,24} In both complexes, the average phenolic C-O bond length is 1.305 Å, which is notably shorter than those of related free ligands, while the average C=N bond distance of 1.285 Å is slightly longer compared to similar free ligands.²² The slight elongation of the C=N bond length, together with the notable shortening of the phenolic C-O distance, may be caused by the tautomeric form of the phenolic hydroxyl group. The average nitrate bite angles lie between 49.49(8)–51.59(6)° in **1** and **2**, while the average bond angle around the *sp*² hybridized azomethine carbon atom is 125.25°.

The crystal structures of the complexes reveal that there exist intra-molecular interactions between the zwitterion proton and the phenolic oxygen (N1-H1...O1, N2-H2...O2 and N3-H3...O3) with donor-acceptor distances ranging from 2.662(2)–2.679(3) Å (see Figure 3 and Table 4). The N2-H2...O51 and N1-H1...O61 interactions represent hydrogen bonds between the zwitterion hydrogens and the nitrate oxygen atoms with lengths of 3.175(3) and 3.147(4) Å in **1** and **2**, respectively. The complexes are further stabilized by C-H...O interactions in the range 3.281(9)–3.493(6) Å. The latter includes interactions between the *tert*-butyl protons and the oxygen atoms of nitrate ions from an adjacent complex within the crystal packing, while other C-H...O interactions occur between the aromatic protons and the nitrate oxygen atoms in the same complex. There are also weak hydrogen bonds observed between the azomethine protons and the oxygen atoms of nitrate ions.

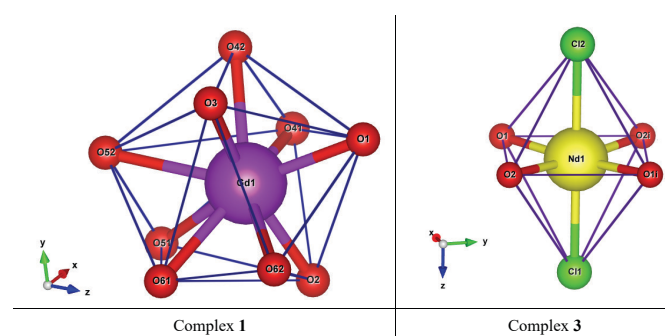
The X-ray crystallographic data reveals the isostructural hexa-coordinate complexes **3–5** with the general formula [Ln(HL₂)₄Cl₂]Cl (Ln = Nd, Gd and Dy) (Figure 3). The complexes crystallized in the orthorhombic *Pnc2* space group system. The coordination spheres around the metal centres consist of four HL₂ molecules binding to the metal in a monodentate manner *via* a phenolic oxygen and two chloride ions. The third chloride ion counters the positive charge on the [Ln(HL₂)₄Cl₂]⁺ moiety. The ChSM values in Table 2 reveal that complexes **3–5** adopt the octahedron (OC-6) geometry, with four oxygen atoms occupying the equatorial positions and the chloride ions occupying the axial positions (Figure 4). An increase in ChSM values as the ionic radius decreases can be attributed to steric crowding around the ion.

In complexes **3–5**, the Ln-O distances range from 2.229(4) to 2.2797(18) Å (Table 3). The average Ln-Cl bond length is 2.6530 Å. The

Table 4: Selected hydrogen bond parameters (Å, °) for **1** and **3**.

	D-H...A	D-H	H...A	D...A	D-H...A
Complex 1	N1-H1...O1	0.85(2)	1.99(3)	2.673(3)	137(3)
	N2-H2...O2	0.86(3)	1.95(3)	2.661(3)	140(3)
	N2-H2...O51	0.86(3)	2.47(3)	3.175(3)	140(3)
	C24-H24A...O51	0.9800	2.5800	3.420(6)	143.00
Complex 3	N1-H1...O1	0.92(6)	1.94(7)	2.633(7)	131(5)
	N2-H2...O2	0.90(6)	2.00(5)	2.664(7)	129(5)
	C11-H11...Cl3 ⁱ	0.9500	2.7000	3.613(5)	162.00
	C21-H21...Cl3	0.9500	2.6100	3.553(5)	170.00
	C23-H23A...Cl2	0.9800	2.8100	3.754(7)	162.00

Note: D = donor, A = acceptor. Symmetry codes: (i) 1+x, y, z.

**Figure 4:** Coordination polyhedrons for the Ln(III) ions in complexes **1** and **3**.

average bond distance of the azomethine group (>C=N<) is 1.2780 Å. The average O1i-Ln-O1 and O2i-Ln-O2, and Cl1-Ln-Cl2 angles are 175.5° and 180.0°, respectively. The slight deviation of the O-Ln-O angles from linearity can be attributed to steric hindrance in the equatorial region. The bond angle around the azomethine carbon (N1-C11-C111 and N2-C21-C211) lies between 122.6(6) and 125.8(7)°.

The crystal packing of **3** and **4** is stabilized by the strong N-H...O_{phenoxo} hydrogen bonds, with bond distances ranging from 2.633(7)–2.670(9) Å (Figure 3; Table 4). In the crystal packing of **5**, the hydrogen bonds are observed between the phenolic proton and the azomethine nitrogen. It is worth noting that the weak C-H...Cl interactions in all the complexes play an important role in stabilising their structures.

CONCLUSION

Five novel complexes described by the general formulae [Ln(HL₂)₃(NO₃)₃] (**1** and **2**) and [Ln(HL₂)₄Cl₂]Cl (**3–5**) were prepared and characterized by the usual physico-chemical techniques including single-crystal X-ray diffractometry. The crystallographic data reveals that the potentially bidentate *N,O*-donor ligand HL₂ coordinated in a monodentate manner to the metal ions. The molecular structures of **1** and **2** reveals that their coordination spheres consist of three HL₂ ligands bonded to the metal centres *via* the phenolate oxygen and three nitrate ions; the latter coordinated in a bidentate manner and the complexes adopted a muffin (MFF-9) geometry.

Complexes **3–5** adopted a distorted octahedral geometry with the coordination environment around each metal centre consisting of four monodentate neutral ligands. In complexes **1–4** the phenolic proton migrated to the azomethine nitrogen atom to form a zwitterion; however, in **5** phenolic proton migration did not occur.

SUPPLEMENTARY DATA

Supplementary information for this article is provided in the online supplement. Crystallographic data for the reported complexes **1–5**

have been deposited at the Cambridge Crystallographic Data Centre with CCDC reference numbers 2042820–2042824, respectively. These data are available from the CCDC, 12 Union Road, Cambridge CB2 1EZ, UK on request or can be obtained free of charge from the Cambridge Crystallographic Data Centre via <https://www.ccdc.cam.ac.uk/structures>.

ACKNOWLEDGEMENTS

This research was supported by the National Research Foundation (unique grant number: 106004).

ORCID IDs

Eric C. Hosten – <https://orcid.org/0000-0003-4173-2550>

Abubak'r Abrahams – <https://orcid.org/0000-0003-0096-0047>

Tatenda Madanhire – <https://orcid.org/0000-0001-6352-183X>

REFERENCES

1. Khalil MMH, Aboaly MM, Ramadan RM. Spectroscopic and electrochemical studies of ruthenium and osmium complexes of salicylideneimine-2-thiophenol Schiff base. *Spectrochim Acta A Mol Biomol Spectrosc.* 2005;61(1-2):157–161. doi:10.1016/j.saa.2004.03.015.
2. Sobola AO, Watkins GM, van Brecht B. Synthesis, characterization and antimicrobial activity of copper(II) complexes of some ortho-substituted aniline Schiff bases; Crystal structure of bis(2-methoxy-6-imino) methylphenol copper(II) complex. *S Afr J Chem.* 2014;67:45–51.
3. Kumar PP, Rani BL. Synthesis and characterization of new Schiff bases containing pyridine moiety and their derivatives as antioxidant agents. *Int J Chemtech Res.* 2011;3:155–160.
4. Cozzi PG. Metal–Salen Schiff base complexes in catalysis: practical aspects. *Chem Soc Rev.* 2004;33(7):410–421. doi:10.1039/B307853C.
5. Chen P, Li Q, Chen S, Yan P, Wang Y, Li G. NIR luminescence of 2-(2'-hydroxyphenyl)benzimidazole lanthanide (Ln=Nd and Yb) complexes. *Inorg Chem Commun.* 2012;17:17–20. doi:10.1016/j.inoche.2011.12.005.
6. Khorshidifard J, Rudbari HA, Askari B, Sahihi M, Farsani MR, Jalilian F, Bruno G. Cobalt(II), copper(II), zinc(II) and palladium(II) Schiff base complexes: Synthesis, characterization and catalytic performance in selective oxidation of sulfides using hydrogen peroxide under solvent-free conditions. *Polyhedron.* 2015;95:1–13. doi:10.1016/j.poly.2015.03.041.
7. Zou X, Yan P, Zhang J, Zhang F, Hou G, Li G. NIR luminescence and catalysis of multifarious salen type ytterbium complexes modulated by anions. *Dalton Trans.* 2013;42(36):13190–13199. doi:10.1039/c3dt51556g.
8. Liu C, Qian Q, Nie K, Wang Y, Shen Q, Yuan D, Yao Y. Lanthanide anilido complexes: synthesis, characterization, and use as highly efficient catalysts for hydrophosphonylation of aldehydes and unactivated ketones. *Dalton Trans.* 2014;43(22):8355–8362. doi:10.1039/c4dt00522h.
9. Bruker APEX. 2 & SAINT. Madison, Wisconsin, USA: Bruker AXS Inc.; 2010.
10. Spek AL. Structure validation in chemical crystallography. *Acta Crystallogr.* 2009;D65:148–155.
11. Sheldrick GM. A short history of SHELX. *Acta Crystallogr A.* 2008;64(1):112–122. doi:10.1107/S0108767307043930.
12. Farrugia LJ. ORTEP-3 for Windows - a version of ORTEP-III with a graphical user interface (GUI). *J Appl Cryst.* 1997;30(5):565. doi:10.1107/S0021889897003117.
13. Pinsky M, Avnir D. Continuous symmetry measures. 5. The classical polyhedra. *Inorg Chem.* 1998;37(21):5575–5582. doi:10.1021/ic9804925.
14. Geary WJ. The use of conductivity measurements in organic solvents for the characterisation of coordination compounds. *Coord Chem Rev.* 1971;7(1):81–122. doi:10.1016/S0010-8545(00)80009-0.
15. Chikate RC, Bajaj HA, Kumbhar AS, Kolhe VC, Padhye SB. Thermal and spectral properties of lanthanide(III) complexes of 3-amino-2-hydroxy-1,4-naphthoquinone. *Thermochim Acta.* 1995;249:239–248. doi:10.1016/0040-6031(95)90702-5.
16. Tiyapiboonchaiya C, Pringle JM, Sun J, Byrne N, Howlett PC, Macfarlane DR, Forsyth M. The zwitterion effect in high-conductivity polyelectrolyte materials. *Nat Mater.* 2004;3(1):29–32. doi:10.1038/nmat1044.
17. Pui A, Malutan T, Tataru L, Malutan C, Humelnicu D, Carja G. New complexes of lanthanide Ln(III), (Ln = La, Sm, Gd, Er) with Schiff bases derived from 2-furaldehyde and phenylenediamines. *Polyhedron.* 2011;30(12):2127–2131. doi:10.1016/j.poly.2011.05.029.
18. Mohamed GG, Sharaby CM. Metal complexes of Schiff base derived from sulphametrole and *o*-vanillin. Synthesis, spectral, thermal characterization and biological activity. *Spectrochim Acta A Mol Biomol Spectrosc.* 2007;66(4-5):949–958. doi:10.1016/j.saa.2006.04.033.
19. Terazzi E, Rivera J-P, Ouali N, Piguët C. A justification for using NMR model-free methods when investigating the solution structures of rhombic paramagnetic lanthanide complexes. *Magn Reson Chem.* 2006;44(5):539–552. doi:10.1002/mrc.1790.
20. Sun W-B, Yan P-F, Li G-M, Xu H, Zhang J-W. *N,N'*-bis (salicylidene) propane-1, 2-diamine lanthanide (III) coordination polymers: Synthesis, crystal structure and luminescence properties. *J Solid State Chem.* 2009;182(2):381–388. doi:10.1016/j.jssc.2008.11.016.
21. Zhao G, Feng Y, Wen Y. Syntheses, crystal structures and kinetic mechanisms of thermal decomposition of rare earth complexes with Schiff base derived from *o*-vanillin and *p*-toluidine. *J Rare Earths.* 2006;24(3):268–275. doi:10.1016/S1002-0721(06)60107-5.
22. Gao T, Yan P-F, Li G-M, Zhang J-W, Sun W-B, Suda M, Einaga Y. Correlations between structure and magnetism of three *N,N'*-ethylene-bis(3-methoxysalicylideneimine) gadolinium complexes. *Solid State Sci.* 2010;12(4):597–604. doi:10.1016/j.solidstatesciences.2010.01.010.
23. Piguët C, Galdes CFGC. Chapter 215. Paramagnetic NMR lanthanide induced shifts for extracting solution structures. In: Gschneidner KA, Bünzli J-CG, Pecharsky VK, editors. *Handbook on the Physics and Chemistry of Rare Earths.* Vol. 33. Amsterdam, Netherlands: Elsevier Science B.V.; 2003. p. 356.
24. Zhou J, Wang L-F, Wang J-Y, Tang N. Synthesis, characterization, antioxidative and antitumor activities of solid quercetin rare earth(III) complexes. *J Inorg Biochem.* 2001;83(1):41–48. doi:10.1016/S0162-0134(00)00128-8.